Available online at www.pelagiaresearchlibrary.com

Pelagia Research Library

Advances in Applied Science Research, 2012, 3 (5):2847-2859

ISSN: 0976-8610
CODEN (USA): AASRFC

Performance of lightweight thin-walled steel sections: theoretical and mathematical considerations

Carine Louise Nilsen[1], Md Azree Othuman Mydin[2] and Mahyuddin Ramli[2]

[1]Department of Civil and Environmental Engineering, University of Illinois at Urbana-Champaign 205 North Mathews Ave., Urbana, IL 61801-2352, USA
[2]School of Housing, Building and Planning, Universiti Sains Malaysia, 11800, Penang, Malaysia

---

ABSTRACT

Globally, thin-walled steel sections have been extensively employed as prime load-bearing members, such as wall studs, floor joints, columns and beams, in low to medium-rise buildings such as offices, hotels, flat blocks and houses. In spite of the accessibility of steel sections, there are still vital barriers that restrain its recognition and execution in the construction industry. Perhaps one of the major barriers is that the building industry is in general disinclined to execute alternative building methods and materials unless it demonstrates obvious and comprehensible quality or performance benefits. It can be found that the behaviour of thin-walled steel sections, including local buckling, distortional buckling, global buckling and shear buckling have been well understood and appropriate design methods existed. The theoretical and mathematical equations presented in this paper will aid future researchers in designing satisfactory thin-walled steel structures holistically.

Keywords: thin-walled, steel section, lightweight framing, local buckling, distortional, mathematical model, global buckling, shear buckling

---

INTRODUCTION

During the last years, thin-walled steel section construction has been a serious rival to the more traditional wood frame system and has gained ground all over the world, particularly in Europe countries, Australia, Canada, United States and some Asian countries for application in low rise residential and commercial constructions. The reason for this growing application of thin-walled steel is primarily based on several advantages deriving from high strength to weight ratio, high stiffness, easy erection and installation compared to thicker hot-rolled steel members, homogeneous quality, termite proof and non-combustibility. The main structural components utilized for housing are roof rafters, decks, wall studs, slab joists, ceiling joists, and roof trusses. In spite of the availability of cold-formed steel system, there are still crucial barriers that hold back its acceptance and implementation in the construction industry. Perhaps one of the prime obstacles is that the building industry is in general disinclined to implement alternative building methods and materials unless it demonstrates apparent and understandable quality or performance benefits.

Given that thin-walled sections are slender; this will increase the behavioural occurrences, which are not regularly found in the hot-rolled sections system. First of all, when thin-walled sections are exposed under compression, local buckling will take place because the plate width to thickness ratio is very high. This local buckling effect will diminish the member stiffness against overall flexure and torsion. Fig. 1 demonstrates the effect of local buckling in column. Flat elements in compression that have both edges parallel to the direction of stress stiffened by a web, flange, lip or stiffener are referred to as stiffened elements. Secondly, distortional buckling at times occurs in compressed lipped channel sections of intermediate length. Distortional buckling of a lipped channel typically

involves rotation of the flanges and the lips around the flange-web junctions. Figure 2 illustrates the typical distortional buckling mode of a lipped channel sections.

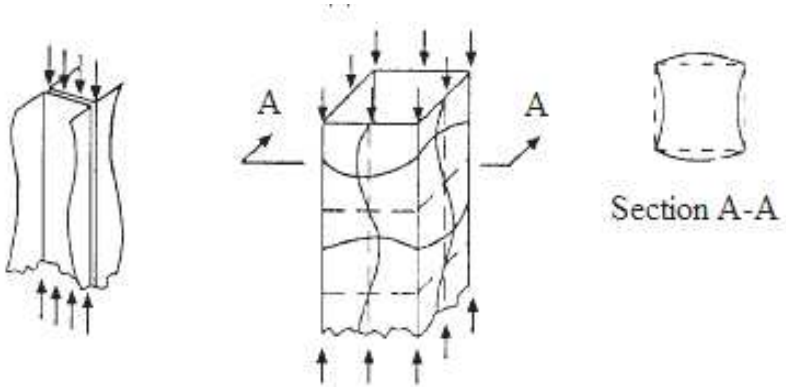

Figure 1. Local buckling of compression elements in column

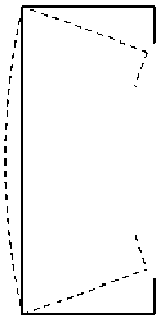

Figure 2. Distortional buckling mode of a lipped channel section

Thirdly, thin-walled steel columns are more simply to fail in flexural buckling as they always have a larger slenderness compared to the same length of hot-rolled columns. Fourthly, given that several thin-walled sections have either no, or only one, axis of symmetry (as shown in Fig. 3), this means that these sections have a natural inclination to twist under load. Thus they will more simply to fail in torsional buckling or flexural-torsional buckling. Finally, a thin-walled steel section may fail in shear buckling owing its small thickness. To sum up, when compared to hot-rolled steel sections, cold-formed thin-walled steel sections are more possible to fail in local buckling, distortional buckling, various global buckling and shear buckling.

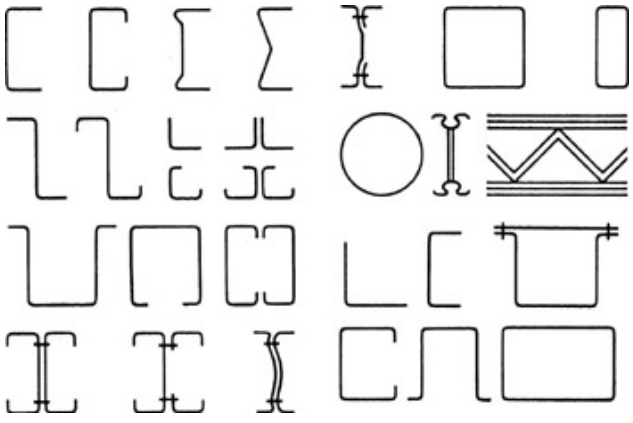

Figure 3: Typical cold-formed steel sections

2. THEORETICAL AND MATHEMATICAL CONSIDERATIONS FOR THIN-WALLED STEEL SECTIONS

2.1 Local buckling

Local buckling is predominantly common in thin-walled sections and is characterised by the fairly short buckling wavelength of individual plate elements. For each plate, the local buckling capability depends on the effective area of the plate, which is equivalent to the effective width of the plate multiplied by its thickness. The effective width of

a plate depends on the stress distribution in the plate, the supporting state and the width to thickness ratio of the plate. Fig. 4 shows the form of stress distribution regularly encountered across the decisive section of a homogeneously compressed plate. The utmost stress occurs at the supported plate edges whilst stresses near the profoundly buckled plate centre are comparatively small, such that it can be considered that the effectiveness of the plate in enduring loading is confined to the supported plate edges. The effective width concept assumes that the portions of a plate element (e.g. $b_{eff}/2$ in Fig. 4) near the supports are completely effective in resisting load and the remainder of the element is completely ineffective as shown in Fig. 4.

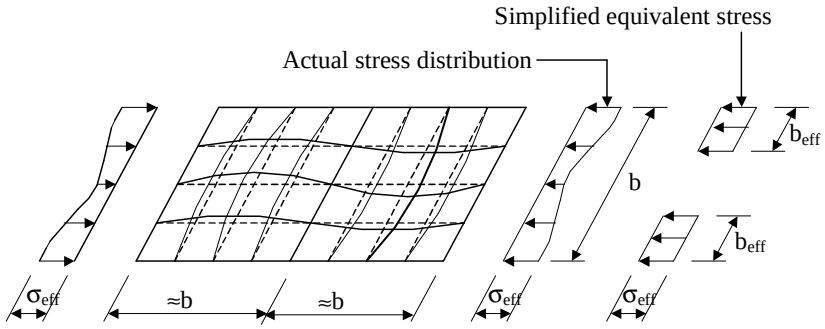

Figure 4: Effective width b_{eff} of a plane element stiffened along both edges.

Winter's equation [1] is typically adopted by different design methods. It gives:

$$\frac{b_{eff}}{b} = 1 \qquad \text{if } \lambda \le 0.673 \tag{1}$$

$$\frac{b_{eff}}{b} = \frac{1}{\lambda}\left(1 - \frac{0.22}{\lambda}\right) \qquad \text{if } \lambda > 0.673 \tag{2}$$

in which the plate slenderness λ is defined by:

$$\lambda = \sqrt{\frac{Y_s}{\sigma_{cr}}} = 1.052\frac{b}{t}\sqrt{\frac{Y_s}{Ek_\sigma}} \tag{3}$$

where, b is the plate width; b_{eff} is the effective width of the plate; σ_{cr} is the critical buckling stress of the plate, and Y_s is the maximum edge stress of the plate and may be taken as the design yield stress of the plate. E is the Young's modulus; k_σ is a buckling factor, which is a function of the plate supporting condition. k_σ = 4.0 for a simply supported plate in uniform compression and 0.43 for an outstand plate element with one edge free.

The expression for effective width in BS5950 Part 5 (1998) is:

$$\frac{b_{eff}}{b} = [1 + 14(\sqrt{\frac{Y_s}{\sigma_{cr}}} - 0.35)^4]^{-0.2} \tag{4}$$

2.2 Distortional buckling

Distortional buckling has only newly received the concentration of researchers and a number of analytical methods have been developed for determining the elastic distortional buckling stress of individually symmetric cross-sections.

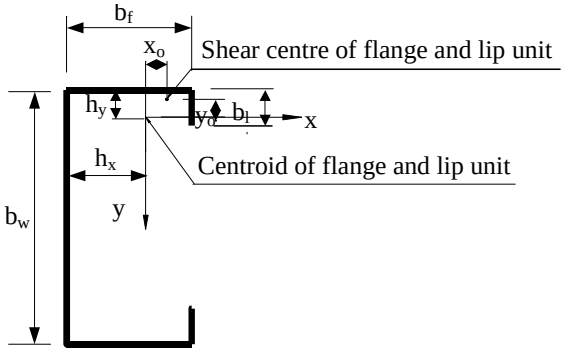

Figure 5. Cross-section of a lipped channel

With reference to Fig. 5, since distortional buckling primarily involves the rotation and lateral bending of the flanges, estimated expressions can be derived by considering the flanges in isolation, assuming that they are undistorted. [2] have given an analytical expression and a straightforward method to calculate the distortional buckling stress of thin-walled lipped channel section columns. The design formulas are shown below:

$$P_{cr} = \frac{E}{2}\{(\alpha_1 + \alpha_2) \pm \sqrt{[(\alpha_1 + \alpha_2)^2 - 4\alpha_3]}\} \quad (5)$$

where, P_{cr} is the distortional buckling load.

$$\alpha_1 = \frac{\eta}{\beta_1}(\beta_2 + 0.039J\lambda^2) + \frac{K_\phi}{\beta_1 \eta E} \quad (6)$$

$$\alpha_2 = \eta(I_y - 2y_0 \frac{\beta_3}{\beta_1}) \quad (7)$$

$$\alpha_3 = \eta(\alpha_1 I_y - \frac{\eta}{\beta_1}\beta_3^2) \quad (8)$$

$$\beta_1 = h_x^2 + \frac{(I_x + I_y)}{A} \quad (9)$$

$$\beta_2 = I_w + I_x(x_0 - h_x)^2 \quad (10)$$

$$\beta_3 = I_{xy}(x_0 - h_x) \quad (11)$$

$$\beta_4 = \beta_2 + (y_0 - h_y)[I_y(y_0 - h_y) - 2\beta_3] \quad (12)$$

$$\lambda = \pi(\frac{E\beta_4 b_w}{2D})^{0.25} = 4.80(\frac{\beta_4 b_w}{t^3})^{0.25} \quad (13)$$

$$\eta = (\frac{\pi}{\lambda})^2 \quad (14)$$

$$K_\phi = \frac{Et^3}{5.46(b_w + 0.06\lambda)}[1 - \frac{1.11P'}{EAt^2}(\frac{b_w^2\lambda}{b_w^2 + \lambda^2})^2] \quad (15)$$

$$P' \text{ is obtained from Eqn. 2.5 with } \alpha_1 = \frac{\eta}{\beta_1}(\beta_2 + 0.039J\lambda^2) \quad (16)$$

$$\text{The distortional stress is } \sigma_{de} = \frac{P_{cr}}{A} \quad (17)$$

In equations 5-17, E is the Young's modulus of steel; D is the lipped flange flexural rigidity, $D = \frac{Et^3}{12(1-\nu^2)}$; ϖ is the Poisson's ratio; I_x and I_y are the second moments of area of the lipped flange about x, y axes, respectively; I_{xy} is the product second moment of area of the lipped flange about the x, y axes; I_w is the warping constant of the lipped flange; J is the torsion constant of the lipped flange; A is the cross-sectional area of the lipped flange; t is the thickness of the flange; b_w is the depth of the web; h_x and h_y are the x, y coordinates of the flange/web junction; x_0 and y_0 are the x, y coordinates of the shear centre, as shown in Fig. 5. In Fig. 5, the origin of the x-y axes is at the centroid of the flange and lip unit.

Kwon and Hancock (1992) reported a series of compression test results on lipped channel sections with fixed ends and proposed two design equations, which may be used to explicitly consider distortional buckling in design calculations. The first is an extension of the earlier equations given by Lau and Hancock (1988) based on the column-buckling philosophy. The formulations are:

$$\sigma_{max} = f_y(1 - \frac{f_y}{4\sigma_{de}}) \quad \text{if } \sigma_{de} \geq \frac{f_y}{2} \quad (18)$$

$$\sigma_{max} = f_y\left[0.055\left(\sqrt{\frac{f_y}{4\sigma_{de}}} - 3.6\right)^2 + 0.237\right] \quad \text{if } \frac{f_y}{13} \leq \sigma_{de} \leq \frac{f_y}{2} \quad (19)$$

where σ_{de} is the elastic distortional buckling stress, given by σ_{de} in equation 17, f_y is the yield stress.

The second is a modification of plate-strength curve and is based mainly on the plate-strength design approach as used for distortional buckling in the AISI specification when the lip is not adequate to fully support the flange [1]. The formulation is given by:

$$\frac{b_{eff}}{b}=1, \quad \lambda \le 0.561 \tag{20}$$

$$\frac{b_{eff}}{b}=(\frac{\sigma_{de}}{f_y})^{0.6}(1-0.25(\frac{\sigma_{de}}{f_y})^{0.6}) , \qquad \lambda \ge 0.561 \tag{21}$$

The distortional buckling slenderness is defined as:

$$\lambda=\sqrt{\frac{f_y}{\sigma_{de}}} \tag{22}$$

These two proposed design equations are consistent when predicting distortional buckling load, but the second one is easier to combine with current code design methods to predict the failure load for mixed local and distortional buckling model including the case where local buckling occurs before distortional buckling.

The generalized Beam Theory (GBT) has become a useful tool to study distortional buckling of thin-walled columns. Davies and Leach [3,4] gave more details. Separate and combined individual buckling modes can be associated with load components in GBT.

The basic equation of GBT is

$$E^kC^kV''''-G^kD^kV''+{}^kB^kV={}^kq \tag{23}$$

in which the second-order effects are excluded. Ignoring the shear effect, the equation for mode 'k' is

$$E^kC^kV''''-G^kD^kV''+{}^kB^kV+\sum_i\sum_j {}^{ijk}k({}^iW^jV')'={}^kq \tag{24}$$

where k denotes mode k; ${}^kC$ is the generalized warping constant; ${}^kD$ is the generalized torsional constant and ${}^kB$ is the transverse bending stiffness. The generalized section properties depend only on the cross-section geometry. ${}^{ijk}k$ is a three dimensional array of second-order terms which takes account of the interactions between in-plane stresses in the faces and out-of-plane deformations. ${}^kV$ and ${}^kW$ are the generalized deformation and warping stress resultants in the i^{th} mode, respectively. E and G are the modulus of elasticity and shear modulus. ${}^kq$ is the uniformly distributed load and n is the number of modes in the analysis. The critical stress ${}^iW$, can be obtained if ${}^kq$ is zero.

If assuming that the member will buckle in a half sine wave of wavelength λ, the critical stress for single-mode buckling, which is valid for buckling in any individual mode, is [4]:

$${}^{i,k}W=\frac{1}{{}^{ijk}k}\left(E^kC[\frac{\pi}{\lambda}]^2+G^kD+{}^kB[\frac{\lambda}{\pi}]^2\right) \tag{25}$$

As the wavelength is varied, the minimum critical stress result is:

$${}^{i,k}W=\frac{1}{{}^{ijk}k}(2\sqrt{E^kC^kB}+G^kD) \tag{26}$$

and the corresponding half-wavelength is

$${}^k\lambda=\pi(\frac{E^kC}{{}^kB})^{0.25} \tag{27}$$

From equations 25, 26 and 27 it can be seen that the distortional critical stress resultant for mode k is only dependant on the second-order coupling term ${}^{ikk}k$ when the load is applied in a different mode i and the half wavelength depends only on the cross-section properties ${}^kC$ and ${}^kB$ which are independent of the load.

[5,6] have carried out a detailed calibration for distortional buckling prediction against more accurate whole-section analysis offered by GBT. They pointed that the rotational restraint stiffness k_ϕ in equation (15) may become negative with increasing depth of the web from equation 15 and if the web buckles earlier than the flange, this may result in a low prediction of the distortional buckling stress. Therefore, for this case, a simple buckling model where the rotational restraint between the flange and the web can be treated as zero can be established and the buckling stresses in the flange and web can be analysed separately. As the buckling load P' of the flange alone can be obtained with k_ϕ taken as zero in equation 15, the buckling stress of the web plate is:

$$\sigma_w = \frac{\pi^2 D}{t b_w^4}\left(\frac{b_w^2 + \lambda^2}{\lambda}\right)^2 \tag{28}$$

When the buckling stress in the web is smaller than that in the flange, there is some buckling interaction and the mean buckling stress can be calculated approximately by:

$$\sigma_{cr} = (2P' + \sigma_w b_w t)/A_g \tag{29}$$

where, A_g is the area of whole cross-section.

In the AISI Specification [7], the failure of the edge stiffener to prevent distortional buckling is considered by reducing the local buckling coefficient of the plate element supported by the stiffener to a value below 4.0. In this method, the buckling coefficient (k_σ) can be chosen from Table 1.

Table 1. Buckling coefficient k to consider distortional buckling effect

	Buckling coefficient k_σ	
	$0.25 < w/b_f \le 0.8$	$w/b_f \le 0.25$
$\frac{w}{t} \le \frac{S}{3}$	4	
$\frac{S}{3} < \frac{w}{t} < S$	$k_\sigma = (4.82 - \frac{5b_L}{w})(\frac{I_s}{I_a})^{0.5} + 0.43 \le 5.25 - \frac{5b_L}{w}$	$k_\sigma = 3.57(\frac{I_s}{I_a})^{0.5} + 0.43 \le 4.0$
$S \le \frac{w}{t}$	$k_\sigma = (4.82 - \frac{5b_L}{w})(\frac{I_s}{I_a})^{1/3} + 0.43 \le 5.25 - \frac{5b_L}{w}$	$k_\sigma = 3.57(\frac{I_s}{I_a})^{1/3} + 0.43 \le 4.0$

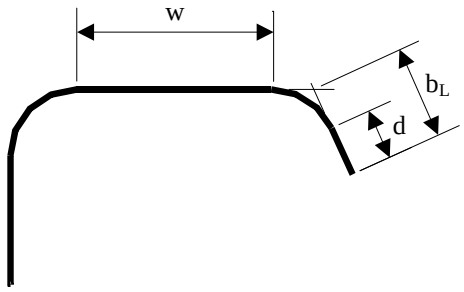

Figure 6. Elements with edge stiffener

In ENV1993-1-3 [9[, distortional buckling is taken into account by assuming that the edges of the intermediate stiffeners where distortional buckling may occur, behave as compressed struts on elastic foundations. The elastic foundation is represented by a spring whose stiffness depends upon the bending stiffness of the adjacent parts to the plate element of the cross-section under consideration and on the boundary condition of the element. The spring stiffness of the stiffener may be determined by applying a unit load per unit length to the cross-section at the location of the stiffener, as illustrated in Fig. 7. The spring stiffness K per unit length may be determined form:

$$K = u/\delta \tag{30}$$

where δ is the deflection of the stiffener due to a unit load u acting in the centroid of b_{e2} and b_{eL}. For an edge stiffener, the deflection can be obtained from;

$$\delta = \theta b_f + \frac{\mu b_f^3}{3} \times \frac{12(1-\nu^2)}{Et^3} \tag{31}$$

with $\theta = \mu b_f / C_\theta$

Therefore, the spring stiffness k can be stated as:

$$K = \frac{Et^3}{4(1-\nu^2)} \cdot \frac{1}{b_1^2 b_w + b_1^3 + 0.5 b_1 b_2 b_w k_f} \tag{32}$$

where, b_1, b_2 are the distance from the web-to-flange junction to the centre of the effective area of the edge stiffener of flange 1 and 2, respectively, as shown in Fig. 7; b_f is the flange width, b_w is the web depth; k_f =0 for a beam in bending, $k_f = \frac{A_{eff\,2}}{A_{eff\,1}}$ for a beam in axial compression, k_f=1 for a symmetric beam.

The critical buckling stress can be derived as:

$$\sigma_{cr} = \frac{2\sqrt{KEI_s}}{A_s} \tag{33}$$

in which, A_s and I_s are the effective cross-sectional area and the second moment of area of the stiffener, as shown in Fig. 8.

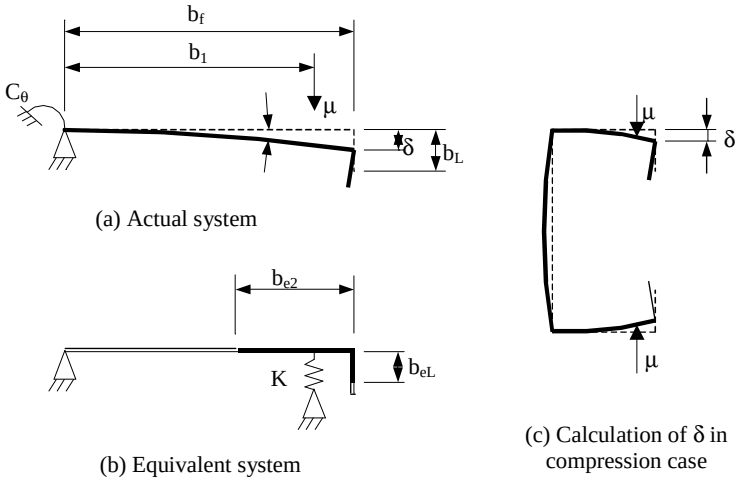

Figure 7. Determination of the spring stiffness K according to ENV1993-1-3 [9]

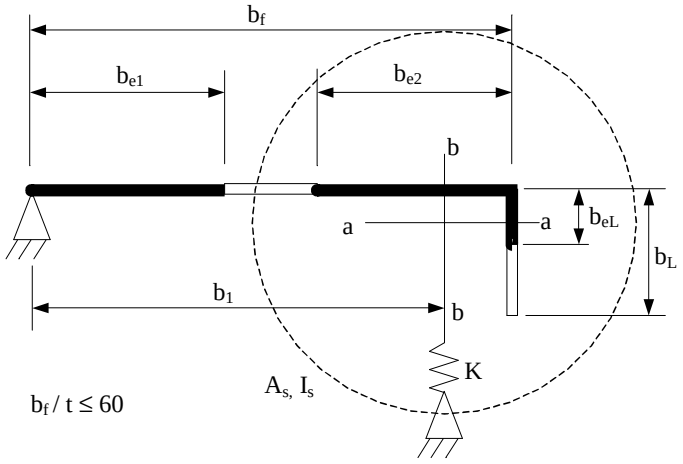

Figure 8.Effective cross-sectional area of an edge stiffener

The rotational stiffness may be expressed as the summation of the elastic and stress-dependent geometric stiffness terms with contributions from the flange and the web, which will be zero if distortional buckling appears. The rotational stiffness may be expressed as:

$$K_\phi = (K_{\phi f} + K_{\phi w})_e - (K_{\phi f} + K_{\phi w})_g = (K_{\phi f} + K_{\phi w})_e - f(\tilde{K}_{\phi f} + \ddot{K}_{\phi w}) = 0 \tag{34}$$

Therefore, the critical buckling stress (σ_{cr}) is

$$\sigma_{cr} = \frac{(K_{\phi fe} + K_{\phi we})}{(\tilde{K}_{\phi f} + \tilde{K}_{\phi w})} \tag{35}$$

where, $K_{\phi fe}$ and $K_{\phi fg}$ are the elastic rotational stiffness of the flange and the geometric rotational stiffness of the flange, repectively; $K_{\phi we}$ and $K_{\phi wg}$ are the elastic rotational stiffness of the web and the geometric rotational stiffness of the web, respectively.

Analytical models are needed for determining the rotational stiffness contributions from the flange and the web. For the flange, cross-sectional distortion is not important; hence the flange is modelled as a column undergoing torsional-flexural buckling. For the web, cross-sectional distortion must be considered, so the web is modelled as a single finite strip. Therefore, the transverse shape function is a cubic polynomial. The longitudinal shape functions of the flange and web are matched by using a single half-sine wave for each. The final rotational stiffness term for the flange and the web are presented as:

$$K_{\phi fe} = \left(\frac{\pi}{L}\right)^4 \left(EI_{xf}(x_{of} - h_{xf})^2 + EC_{wf} - E\frac{I_{xyf}^2}{I_{yf}}(x_{of} - h_{xf})^2 \right) + \left(\frac{\pi}{L}\right)^2 GJ_f \tag{36}$$

$$\tilde{k}_{\phi fg} = \left(\frac{\pi}{L}\right)^2 \left\{ A_f \left[(x_{of} - h_{xf})^2 \left(\frac{I_{xyf}}{I_{yf}}\right)^2 - 2y_0(x_{of} - h_{xf}) \left(\frac{I_{xyf}}{I_{yf}}\right) + h_{xf}^2 + y_{0f}^2 \right] + I_{xf} + I_{yf} \right\} \tag{37}$$

$$K_{\phi we} = \frac{Et^3}{6b_w(1-\nu^2)} \tag{38}$$

$$\tilde{k}_{\phi wg} = \left(\frac{\pi}{L}\right)^2 \frac{tb_w^3}{60} \tag{39}$$

The critical length can also be found and it is a function of the geometric terms. It can be calculated by:

$$L_{cr} = \left\{ \frac{6\pi^4 b_w(1-\nu^2)}{t^3} \left[I_{xf}(x_{0f} - h_{xf})^2 + I_w - \frac{I_{xyf}^2}{I_{yf}}(x_{0f} - h_{xf})^2 \right] \right\} \tag{40}$$

where, E is elastic modulus; G is shear modulus; ν is poisson's ratio; t is the plate thickness; b_w is the web width; L is the distance between restraints which limit rotation of the flange/web junction; A_f is the gross area of the compression flange; I_{xf} and I_{yf} are the second moments of area of the flange along x and y direction, respectively; I_w is warping constant of the flange. x_{of} is x-distance from the flange/web junction to the centroid of the flange; h_{xf} is x-distance from the centriod of the flange to the shear centre of flange, as shown in Fig. 2.9.

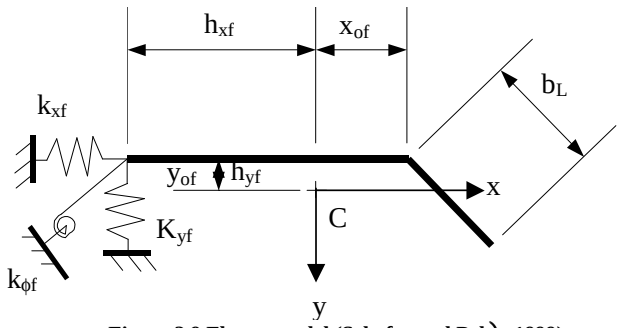

Figure 2.9.Flange model (Schafer and Pekˆz 1999)

Each method for predicting the elastic distortional buckling stress has been compared [9,10]. The method given in ENV 1993-1-3 is quite rough and sometimes gives inaccurate results for C-sections and plates with intermediate stiffness while the method developed by Lau and Hancock [2] correlates better with the results obtained numerically.

2.3 Global buckling

For a thin-walled steel column under compression, the column may undergo different forms of global buckling, including flexural buckling, torsional buckling and combined flexural-torsional buckling. The local buckling and

distortional buckling cause reduction in the effective stiffness of the member and thus affect the overall flexural and torsional-flexural buckling strength of the columns and lateral buckling strength of the beams. Therefore, the ultimate failure of a thin-walled column under compression may be a combination of local and overall buckling or distortional and overall buckling. In design calculations, local and distortional bucking modes are considered first by evaluating the effective cross-section of the structural member. Global buckling is then checked using properties of the effective cross-section, which are obtained from local or distortional buckling behaviour.

Due to local and distortional buckling, the centroid of the effective cross-section and the gross cross-section may not coincide. In this situation, the effect of a shift in the centroid should be included, which can be seen in Fig. 10. This shift in neutral axis is to introduce a bending moment in an axially loaded member.

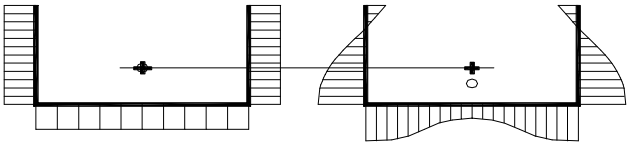

Figure 10.Neutral axis shift

In BS5950 [11], for sections symmetrical about both principal axes or closed cross-sections which are not subject to torsional flexural buckling, or are braced against twisting or columns with fixed end conditions, the flexural buckling load may be calculated as:

$$P_c = 0.5(\{P_{cs} + (1+\eta)P_E\} - [\{P_{cs} + (1+\eta)P_E\}^2 - 4P_{cs}P_E])^{1/2} \quad (41)$$

$$P_E = \frac{\pi^2 EI}{L_e^2} \quad (42)$$

$$\eta = 0.002(L_e / i - 20) \quad (43)$$

In which, P_{cs} is the cross-sectional capacity for local buckling; I is the second moment of area of the cross section; L_e is the effective length of the member; i is the radius of gyration of the gross cross-section corresponding to P_E.

For cross-sections with a single symmetry axis, the effects of movement of the effective neutral axis should be taken into account. The ultimate load carrying capacity for flexural buckling should be calculated as:

$$P_c' = \frac{M_c P_c}{(M_c + P_c e_s)} \quad (44)$$

where M_c is the elastic bending moment capacity of the cross-section, P_c is the flexural buckling capacity in which the neutral axis shit has not been considered and e_s is the distance between the geometric neutral axis of the gross cross-section and that of the effective cross-section .

In 1993-1-3 [8], different buckling curves, which should be chosen in accordance with the type of cross-section and axis of buckling, should be used to determine the flexural buckling capacity.

$$P_c = \chi A_{eff} f_y / \gamma_{M1} \quad (45)$$

$$A_{eff} = \Sigma t b_{eff} = \Sigma t \rho b = \beta_A A \quad (46)$$

$$\chi = \frac{1}{\phi + [\phi^2 - \overline{\lambda}^2]^{0.5}} \quad (47)$$

$$\overline{\lambda} = (\lambda/\lambda_1)[\beta_A]^{0.5} \quad (48)$$

$$\lambda = L_e/i \quad (49)$$

$$\lambda_1 = \pi[E / f_Y]^{0.5} \quad (50)$$

In AISI, the basic equation (51) can be used to determine the various global buckling load.

$$P_c = A_{eff} F_n \quad (51)$$

where, F_n is determined as: $F_n = f_y(1 - f_y / 4F_e)$ for $F_e > f_y / 2$ and $F_n = F_e$ for $F_e \le f_y / 2$ (52)

For flexural buckling, F_e is

$$F_e = \frac{\pi^2 E}{(L_e / i)^2} = \frac{\pi^2 E}{(KL / i)^2} \quad (53)$$

where, A_{eff} is the effective area of the cross-section and K is the effective length factor, which is related to the boundary condition.

If the cross-section of a column has only one axis of symmetry and without lateral bracing against twisting, the column may fail into torsional or torsional buckling mode. The load carrying capacity for torsional or torsional-flexural buckling in BS5950 Part 5 (BSI 1998) can be calculated as:

$$P_c = 0.5(\{P_{cs} + (1+\eta)P_{TF}\} - [\{P_{cs} + (1+\eta)P_{TF}\}^2 - 4P_{cs}P_{TF}]^{1/2} \quad (54)$$

$$P_{TF} = 0.5(\{P_{EX} + P_T\} - [\{P_{EX} + P_T\}^2 - 4\beta P_{EX} P_T]^{1/2} / \beta \quad (55)$$

$$P_{EX} = \frac{\pi^2 E I_X}{L_e^2} \quad (56)$$

$$P_T = \frac{1}{i_0^2}(GJ + 2\frac{\pi^2 E C_w}{L_e^2}) \quad (57)$$

$$\beta = 1 - (\frac{x_0}{i_0})^2 \quad (58)$$

$$i_0 = (i_x^2 + i_y^2 + x_0^2)^{0.5} \quad (59)$$

$$\eta = 0.002(\alpha L_e / i - 20) \quad (60)$$

$$\text{for } P_{EY} > P_{TF}, \quad \alpha = (\frac{P_{EY}}{P_{TF}})^{1/2} \quad (61)$$

$$\text{for } P_{EY} < P_{TF} \quad \alpha = 1 \quad (62)$$

In which, I_x is the second moment of area about the x axis; G is the shear modulus; J is the St Venant torsion constant for the cross-section which may be taken as the summation of $bt^3/3$ for all element, where b is the element flat width and t is the thickness; C_w is the warping constant for the cross-section; x_0 is the distance from the shear centre to the centroid measured along the x axis and i_x and i_y are the gyration about the x and y axes, respectively.

In ENV1993-1-3 [8], buckling curve b is used to determine the torional or torsional-flexural buckling capacities. The basic equation is the same as Eqn. 45, provided coefficient χ is decided as:

$$\chi = \frac{1}{\phi + [\phi^2 - \overline{\lambda}^2]^{0.5}} \quad (63)$$

$$\overline{\lambda} = (f_Y / \sigma_{cr})^{0.5}[\beta_A]^{0.5} \quad (64)$$

$$\sigma_{cr} = \sigma_{cr,TF}, \text{ but } \sigma_{cr} \le \sigma_{cr,T} \quad (65)$$

$$\text{For torsional buckling, } \sigma_{cr,T} = \frac{1}{A_g i_0^2}[GJ + \frac{\pi^2 E C_w}{L_e^2}] \quad (66)$$

in which, the calculation of i_o can be seen in equation 58.

For torsional-flexural buckling, $\sigma_{cr,TF} = \frac{1}{2\beta}[(\sigma_{cr,x} + \sigma_{cr,T}) - \sqrt{(\sigma_{cr,x} + \sigma_{cr,T})^2 - 4\beta\sigma_{cr,x}\sigma_{cr,T}}]$ (67)

$$\sigma_{cr,x} = \pi^2 E / (l_e / i_x)^2 \quad (68)$$

In AISI (1996), the basic equation 51 is also been used to determine the ultimate torsional-flexural buckling capacity. F_e can be calculated as:

$$F_e = \frac{1}{2\beta}[(\sigma_{cr,x} + \sigma_{cr,T}) - \sqrt{(\sigma_{cr,x} + \sigma_{cr,T})^2 - 4\beta\sigma_{cr,x}\sigma_{cr,T}}] \quad (69)$$

where, $\sigma_{cr,x}$ and $\sigma_{cr,T}$ can be calculated by using equations 2.66 and 2.68, respectively.

Some compression members are also subjected to bending and the lateral buckling capacity should be checked. Equations 70-71 have been used to check the lateral buckling capacity in BS5950 Part 5 (BSI 2000).

$$\frac{N_c}{P_C} + \frac{M_X + \Delta M_x}{C_{bx} M_{x,eff}(1 - \frac{F_c}{P_{EX}})} + \frac{M_Y + \Delta M_y}{C_{bY} M_{y,eff}(1 - \frac{N_c}{P_{EY}})} \leq 1 \quad (70)$$

$$\frac{N_C}{P_C} + \frac{M_X + \Delta M_x}{M_{cr}} + \frac{M_Y + \Delta M_y}{C_{bY} M_{y,eff}(1 - \frac{N_C}{P_{EY}})} \leq 1 \quad (71)$$

in which, M_{cr} is the elastic lateral buckling resistance moment; $M_{x,eff}$ is the elastic bending moment capacity of the cross-section about the x axis in the absence of N_c and M_y; $M_{y,eff}$ is the bending moment capacity of the cross-section about y axis in the absence of N_c and M_X; C_{bx},C_{by} are the coefficient defining the variation of moments along x and y axis; N_c is the axial compression load, M_x and M_y are the bending moment about x, y axis, respectively; ΔM_x and ΔM_y are the additional bending moments about the x-x and y-y axes due to neutral axis shifts.

When using ENV1993-1-3 (2001), a beam-column should satisfy the following equations 72-73.

$$\frac{N_C}{\chi_{min} f_y A_{eff} / \gamma_{M1}} + \frac{k_y(M_X + \Delta M_x)}{f_y W_{eff,x,com} / \gamma_{M1}} + \frac{k_Z(M_y + \Delta M_y)}{f_y W_{eff,y,com} / \gamma_{M1}} \leq 1 \quad (72)$$

$$\frac{N_C}{\chi_{lat} f_y A_{eff} / \gamma_{M1}} + \frac{k_{LT}(M_X + +\Delta M_x)}{\chi_{LT} f_y W_{eff,x,com} / \gamma_{M1}} + \frac{k_Z(M_y + \Delta M_y)}{f_y W_{eff,y,com} / \gamma_{M1}} \leq 1 \quad (73)$$

in which, χ_{min} is the less of χ_y and χ_x, where χ_y and χ_x are the reduction factors of buckling about y and x axis; χ_{lat} is the reduction factor for lateral torsional buckling; k_x and k_y are modification factors to account for bending moment distributions in the column about the x-x and y-y axes; $W_{eff,x,com}$ and $W_{eff,y,com}$ are the elastic modulus of the effective section.

3. THIN-WALLED STEEL WALL-STUDS

The diaphragm bracing of steel wall-studs using gypsum boards and other materials was investigated by Simaan and Pekz [12]. They used an energy approach including the shear rigidity and rotational restraint of the diaphragm to develop a design procedure and approximate solution for the buckling of diaphragm-braced wall-studs. The AISI [7] Specification is based on this research. The maximum load that can be carried by wall-studs is governed by column buckling between fasteners in the plane of the wall, flexural and/or torsional overall column buckling out-of-plane, and shear failure of the sheathing. According to AISI [7], it can be found that increased stud spacing increases the overall shear rigidity and results in increased strength prediction for both the overall diaphragm-braced buckling modes and shear failure of the sheathing itself. However, buckling between fasteners is independent of stud spacing. Miller *et al* (1994b) studied the behaviour of gypsum-sheathed cold-formed steel wall studs based on experimental analysis. They found that increasing wallboard thickness and the edge distance to the fastener would increase the failure load per fastener and the failure mode would change from wallboard cracking and tearing to shearing of the screws. They also pointed out that the test results contradicted with the shear-diaphragm model, the deformations of gypsum wallboard panels (in tension) were localized at the fasteners and not distributed throughout the panel. This research led to the imposition of some limitations (e.g. maximum stud spacing) by AISI [7].

[10] studied the behaviour of gypsum-sheathed perforated steel wall studs based on the stud column tests and wall stud assembly tests. They found that the gypsum board connection improved the in-plane buckling resistance but it could not fully restrain the rotation of the flange and the lip. Their calculated strength values according to ENV1993-1-3 [8] are about 20% conservative for the interaction of compression and bending moment if the stud is assumed laterally braced and rotational support of the fasteners is ignored. They concluded that these support conditions may be used in design and would be on the safe side.

[13] presented details of tests of a total of 20 full-scale wall frames, four being unlined, eight being lined on one side while the remaining eight being lined on both sides. Each panel consisted of three studs spaced at 600 or 300mm. The height of the frames was set at 2.4m. For the lined frames, 10mm plasterboard was used. They found that the plasterboard lining should be fastened to the studs at smaller spacing to be able to gain any additional strength. The AISI method is unable to predict the failure mode of some cases and is inadequate in predicting the failure loads of studs lined on one side.

[14] used differential equations of equilibrium to derive a mathematical method to calculate the axial strength (flexural and flexural-torsional buckling loads) for gypsum-sheathed cold-formed steel wall stud composite panels. In their analysis, axial load was assumed to be applied to the centroid of the gross cross-section of each C-shaped stud with bracing action of the wallboard and connection of screws were presented by elastic springs. Their formulations predicted that the panel strength was independent of stud spacing but reflected the localized nature of the wallboard deformation.

[15] reported 30 panels tests, in which 20 panels had only one stud and 10 panels with two studs. The screw spacing was 300mm, 400mm and 600mm in the studs. The boards were oriented strand board (OSB), cement particle board (CPB) and calcium silicate board (CSB). The number of boards used in their tests had no sheathing, one-side or two side sheathing. One point, two point or four point loads were applied on the top of the panel. After tests, all specimens without board sheathing failed in overall flexural buckling. For the panels with one-side sheathing, nearly all of the studs failed as a result of torsional-flexural buckling and the side studs failed due to flexural buckling and heavy local buckling. For the panels with two-side sheathing, the studs failed by overall torsional-flexural buckling and local crushing near their ends. They also found that the board type and number and screw spacing affected the panel load carrying capacities. The failure loads of panels sheathed with OSB were about 20% higher than panels sheathed with CPB and 70% higher than CSB. The failure loads of panels with both side sheathing panels were significantly higher than one-side sheathing panels. The load carrying capacity of studs increases with decreasing screw spacing.

CONCLUSION

This paper has presented thoroughly the theoretical and mathematical considerations for thin-walled steel sections including the studies of the behaviour of thin-walled steel structures at room temperature. It can be found that the behaviour of thin-walled steel structures at room temperature, including local buckling, distortional buckling, global buckling and shear buckling have been well understood and suitable design methods existed. The theoretical and mathematical equations presented in this paper will assist future researchers in designing acceptable thin-walled steel structures holistically.

Acknowledgement
The authors would like to thank Universiti Sains Malaysia and Ministry of Higher Education Malaysia for their financial supports under Fundamental Research Grant Scheme (FRGS). No. 203/PPBGN/6711256.

REFERENCES

[1] Winter, G., Strength of thin-steel compression flanges. Cornell University Eng. Exp. Stn. Report No. 32, **1947**.
[2] Lau, S. C. W., Hancock, G. J., J. of Structural Engineering, ASCE, **1987**, 113:1063-1078.
[3] Davies, J. M., Leach P., J. of Constructional Steel Research, **1994**, 31:187-220.
[4] Davies, J. M., Leach P., J. of Constructional Steel Research, **1994**, 31:221-241.
[5] Davies, J. M., Jiang, C., Non-linear buckling analysis of thin-walled metal columns, Proceeding of Thirteenth International Specialty Conference on Cold-formed Steel Structures, St. Louis, Missouri, U.S.A., **1996**, 321-334.
[6] Davies, J. M., Jiang, C., J. of Constructional Steel Research, **1998**, 46:174-175
[7] AISI, The specification for the design of cold-formed steel structural members, Washington DC: American Iron and Steel Institute, **1996**
[8] CEN, ENV 1993-1-3, Eurocode 3: Design of steel Structures, Part 1.3: General rules, supplementary rules for cold formed thin gauge members and sheeting, European Commission for Standardisation, Brussels, **2001**.
[9] Kesti J., Davies J. M., Thin-walled Structures, **1999,** 32:115-134
[10] Kesti J., Local and distortional buckling of perforated steel wall studs, PhD Thesis, Helsinki University of Technology, Laboratory of Steel Structures, Espoo, **2000**.
[11] BSI, British Standard: Structural use of steelwork in building, Part 5: Code of practice for design of cold formed thin gauge sections, British Standard Institution, **1998**.
[12] Simaan, A.,Pekz, T., J. of Structural Division, **1976**, 102:77-92
[13] Telue, Y., Mahendran, M., J. of Constructional Steel Research, **2001**, 57:435-452.

[14] Lee. J., Mahendran, M., Buckling behaviour of thin-walled compression members at elevated temperatures, Proceedings of the Sixth Pacific Structural Steel conference, Beijing, China, **2001**, 634-641.
[15] Tian, Y. S., Lu, T. J. Barlow, C. Y., Evans, J., An experimental study on the load carrying capacity of cold-formed steel studs and panels, Proceeding of Sixteeth International Specialty Conference on Cold-formed Steel Structures, **2002**, 433-449.